Site-dependent magnetism of Ni adatoms on MgO/Ag(001)

Oliver R. Albertini* and Amy Y. Liu
Department of Physics, Georgetown University, Washington, DC 20057, USA

Barbara A. Jones
IBM Almaden Research Center, San Jose, CA 95120, USA

(Dated: April 6, 2015)

We examine the adsorption of a single Ni atom on a monolayer of MgO on a Ag substrate using DFT and DFT+U computational approaches. We find that the electronic and magnetic properties vary considerably across the three binding sites of the surface. Two of the binding sites are competitive in energy, and the preferred site depends on the strength of the on-site Coulomb interaction U. These results can be understood in terms of the competition between bonding and magnetism for surface adsorbed transition metal atoms. Comparisons are made with a recent experimental and theoretical study of Co on MgO/Ag, and implications for scanning tunneling microscopy experiments on the Ni system are discussed.

PACS numbers: 73.20.Hb, 75.70.Rf

I. INTRODUCTION

The study of magnetic adatoms on surfaces has drawn recent attention due to possible applications in the realm of magnetic storage and quantum computation. The density of magnetic storage has enjoyed exponential growth for several decades, but this growth will eventually slow as particle sizes approach the superparamagnetic regime.[1] An alternative, bottom-up approach is to start from the atomic limit. With the scanning tunneling microscope (STM), single atoms can be moved around on a surface to construct desired nanostructures, and the STM can also be used to probe the electronic and magnetic properties of those nanostructures. Such experiments have found, for example, that a single Fe atom on a Cu_2N monolayer (ML) on Cu has a large magnetic anisotropy energy,[2] and that a magnetic bit consisting of an array of 12 Fe atoms on the same surface has a stable moment that can stay in the 'on' or 'off' state for hours at cryogenic temperatures (~ 1 K).[3]

A recent STM study of a single Co atom on a ML of MgO on the Ag(001) surface found that the Co atom maintains its gas phase spin of $S = 3/2$, and, because of the axial properties of the ligand field, it also maintains its orbital moment on the surface ($L = 3$). The resulting magnetic anisotropy is the largest possible for a $3d$ transition metal, set by the spin-orbit splitting and orbital angular momentum. The measured spin relaxation time of 200 μs is three orders of magnitude larger than typical for a transition-metal atom on an insulating substrate.[4]

Here we investigate the structural, electronic, and magnetic properties of Ni adatoms on the same substrate, MgO/Ag(001), using density functional methods. Previous authors[5–12] have studied the adsorption of transition metal atoms on an MgO substrate using ab-initio techniques. These studies, which employed various surface models and approximations for the exchange-correlation functional, are in general agreement that the preferred binding site of a Ni adatom on the MgO(001) surface is on top of an O atom, and that structural distortion of the MgO surface upon Ni adsorption is minimal. The situation is less clear when it comes to the spin state of the adatom, since the s-d transition energy is so small in Ni. Calculations that employ the generalized gradient approximation for the exchange-correlation functional generally predict a full quenching of the Ni moment on MgO, while partial inclusion of Fock exchange as in the B3LYP hybrid functional predicts that the triplet spin state is slightly more favorable.[7–9]

The system studied in the current work differs from previous studies of Ni adsorption on MgO because the substrate consists of a single layer of MgO atop the Ag(001) surface. This aligns more closely with STM experiments that use a thin insulating layer to decouple the magnetic adatom from the conducting substrate that is necessary for electrically probing the system. We show that, in contrast to the surface layer of an MgO substrate, the MgO ML on Ag can deform significantly due to interactions with the Ni, resulting in a very different potential energy surface for adsorption. Further, we investigate how the interaction of Ni with the MgO/Ag substrate is affected by on-site Coulomb interactions and find that the preferred binding site depends on the interaction strength U. Unlike the case of Co adatoms on the MgO/Ag substrate, the Ni spin moment is always lower than that of the isolated atom. The degree to which the moment is reduced depends strongly on the binding site. These results can be understood by considering the Ni $3d$-$4s$ hybrid orbitals that participate in bonding at different sites. We conclude with a discussion about experiments that could corroborate our findings.

II. METHOD

A. Computational methods

Two sets of density-functional-theory (DFT) calculations were carried out, one using the linearized augmented plane wave (LAPW) method as implemented in WIEN2K,[13] and the other using the projector augmented wave (PAW) method[14] in the VASP package.[15] Both started with the Perdew, Burke and Ernzerhof formulation of the generalized gradient approximation (GGA) for the exchange-correlation functional.[16] In the LAPW calculations, structures for each binding site were relaxed within the GGA. These structures were then used to calculate Hubbard U values for each site using the constrained DFT method of Madsen and Novák.[17] GGA+U calculations were then carried out using those site-specific values of U to examine electronic and magnetic properties, without further structural relaxation. On the other hand, PAW calculations were used to optimize structures within both GGA and GGA+U. However, since the total energy in DFT+U methods depends on the value of the on-site Coulomb interaction strength, the same value of U was used for each adsorption site to allow comparison of binding energies. In all GGA+U calculations, a rotationally invariant method in which only the difference $U - J$ is meaningful was employed.[18]

Within GGA, the two sets of calculations yielded very similar results for adsorption geometries, binding energies, and electronic and magnetic structure, as expected. Although the calculations were used for different purposes in assessing the effect of on-site Coulomb repulsion, the GGA+U results from the two methods were generally consistent and displayed the same trends.[19]

B. Supercell geometry and binding sites

STM experiments require a conducting substrate, yet for magnetic nanostructures, it is desirable to suppress interaction between the adatoms and a metallic substrate. Hence the adatom is often placed on a thin insulating layer at the surface of the substrate. It has been shown experimentally that ultrathin ionic insulating layers can shield the adatom from interaction with the surface.[20] In a recent experimental study of Co adatoms, a single atomic layer of MgO was used as the insulating layer above an Ag substrate.[4,21] The lattice constants of MgO and Ag are well matched (4.19 Å and 4.09 Å, respectively), and DFT calculations of a single layer of MgO on the Ag(100) surface have found that is it energetically favorable for the O atoms in the MgO layer to sit above the Ag atoms.[4]

Here we used this alignment of MgO on Ag(001) in inversion symmetric (001) slabs of at least five Ag layers sandwiched between MLs of MgO. We found only minor differences in results for slabs containing five versus seven Ag layers. The in-plane lattice constant was fixed at the bulk Ag value, and an isolated Ni adatom on the MgO/Ag surface was modeled using a $3/\sqrt{2} \times 3/\sqrt{2}$ supercell of the slab with one Ni atom on each surface, corresponding to a lateral separation of 8.68 Å between adatoms. In the out-of-plane direction, the supercells contained 7 to 8 layers of vacuum.

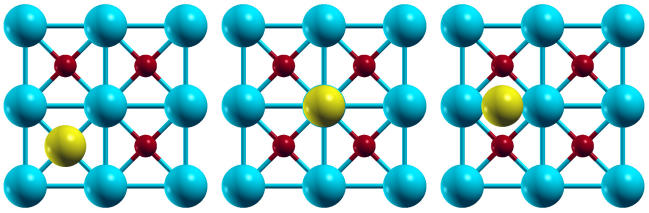

(a) O site (b) Mg site (c) hollow site

FIG. 1. (Color online) Top view of the three binding sites. Cyan spheres represent Mg, small red spheres O, and the yellow spheres Ni.

Three high-symmetry binding sites on the MgO surface were considered, as shown in Fig. 1: Ni on top of an O atom, Ni on top of an Mg atom, and Ni above the center of the square formed by nearest-neighbor Mg and O sites. These will be referred to as the O site, the Mg site, and the hollow site, respectively.

III. RESULTS & DISCUSSION

A. Binding energetics and geometries

Since GGA and GGA+U do not fully describe important correlation effects in the isolated Ni atom, the calculated binding energies are not as reliable as *differences* in binding energy between different adsorption sites. Figure 2 shows the total energy relative to that of the O site. Within GGA, the O site is slightly favored over the hollow site, while the Mg site is about 1 eV higher in energy. For comparison, we also plot our results for Ni on an MgO substrate. Similar to previous reports,[12] we find that on the MgO substrate, Ni clearly favors the O site, with the hollow and Mg sites lying about 1 and 1.7 eV higher in energy, respectively.

The difference between the potential energy surfaces for Ni adsorption on MgO/Ag versus on MgO can be attributed to the greater freedom that the MgO ML has to deform to accommodate the adatom. The pure MgO substrate remains very flat upon Ni adsorption. When Ni is on the O or Mg site, the displacement of surface atoms is negligible, and when it is on the hollow site, the neighboring O atoms displace out of the plane by about 0.09 Å. The situation is very different for Ni on MgO/Ag. Table I lists the distance between the adatom and its nearest Mg and O neighbors, as well as the vertical displacement Δ_z, of those Mg and O atoms. For each adsorption site, at least one of the neighboring atoms is displaced vertically by more than 0.1 Å. The deformation

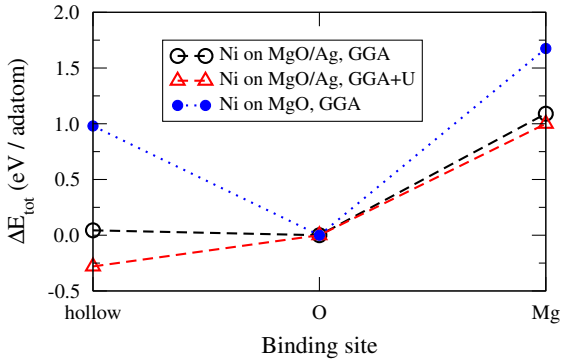

FIG. 2. (Color online) Total energy per Ni adatom on MgO/Ag, calculated for structures relaxed within GGA and GGA+U (U = 4 eV) from PAW calculations. For comparison, energies calculated for Ni adatoms on MgO are also shown. All energies are plotted relative to the O site energy.

of the MgO ML is most striking when Ni is on the hollow site, with neighboring O atoms being pulled up out of the MgO ML by nearly 0.5 Å. This allows the hollow site to be competitive in energy with the O site on MgO/Ag, in contrast to what happens on the MgO surface.

To examine the influence of local correlations on the binding energetics of Ni on MgO/Ag, we present GGA+U results. Since total energies can only be compared for calculations that use the same value of U, structures were relaxed assuming U = 4 eV for all sites. GGA+U predicts that the O and hollow sites reverse order, as shown in Fig. 2. The site above an Mg atom still remains much less favorable than either the O or the hollow site. Of course the Coulomb interaction U depends on the local environment of the Ni atom, so it is an approximation to assume a fixed value for all adsorption sites. Nevertheless, these results demonstrate that on-site correlations can change the preferred adsorption geometry. A similar effect has been reported for the adsorption of 3d transition metals on graphene.[22]

For a Ni adatom above an O atom, the Ni-O bond is weakened by on-site correlations, as evidenced by an increase of about 8% in the Ni-O bond length in going from U = 0 to U = 4 eV. On the hollow and Mg sites, differences between geometries relaxed within GGA and GGA+U are much smaller.

Given the limitations of the DFT+U method, we are not able to definitively predict whether the O site or hollow site is preferred. However, it is likely that the Mg site is uncompetitive, and not experimentally feasible. Hence the remainder of the paper deals primarily with the hollow and O binding sites, comparing their electronic and magnetic properties.

B. Electronic and Magnetic Properties

Based on the geometries relaxed within GGA, our constrained DFT calculations yield Coulomb parameters U = 4.6, 6.0, and 5.0 eV for Ni 3d electrons on the O, hollow, and Mg sites, respectively. The GGA+U results presented in this section use these site-specific values of U, but assume the GGA-relaxed geometries. As mentioned, the O-site geometry is somewhat sensitive to the inclusion of on-site Coulomb repulsion, but the Mg-site and hollow site geometries are not.

Atomic Ni has a ground state configuration of $3d^8 4s^2$ ($^3F_4$) with the next highest state $3d^9 4s^1$, belonging to a different multiplet (^3D), only 0.025 eV away.[23] The average energies of these multiplets, however, have $3d^9 4s^1$ 0.030 eV lower in energy.[23] The proximity of these atomic states sets the stage for a competition between chemical bonding and magnetism.[8]

Our GGA calculations give a $3d^9 4s^1$ ground-state configuration for atomic Ni, which underrepresents the s occupation compared to experiment, while inclusion of a local Coulomb interaction (U = 6.0 eV) yields a $3d^8 4s^2$ configuration. In both cases, the Ni moment is calculated to be 2.0 μ_B.

The calculated magnetic moments for Ni on MgO/Ag are listed in Table II. The Ni spin moment is reduced from the atomic value on all sites, though by varying amounts. When Ni is on the O site, the magnetic moment is calculated to be zero within GGA, but it increases slightly upon inclusion of U. (When the structure is relaxed within GGA+U and the Ni-O bond length increases by 8%, the moment increases to about 0.3 μ_B.) On the hollow site, the magnetic moment of about 1 μ_B is insensitive to U, while the larger moment of about 1.5 μ_B on the Mg site increases with U.

In Table III, we present the results of a Bader charge analysis[24] (space filling) for the adatom and its nearest

TABLE I. Relaxed distance between adatom and nearest-neighbor Mg and O atoms, and height of these atoms above the MgO ML. All distances are in Å. Results were obtained within the GGA using the all-electron LAPW method.

Adatom	Binding site	$d_{\text{ad-O}}$	$d_{\text{ad-Mg}}$	Δz_{O}	Δz_{Mg}
Ni	O site	1.79	2.87	+0.15	+0.06
Ni	hollow site	1.90	2.53	+0.48	−0.18
Ni	Mg site	3.63	2.73	−0.15	+0.20
Co	O site	1.85	2.95	−0.06	−0.20

TABLE II. Total magnetization per adatom (in μ_B) for different sites, calculated within GGA and GGA+U, from all-electron LAPW calculations. Site-specific values of U are listed in eV.

Adatom	Binding site	m_{GGA}	$m_{\text{GGA+}U}$	U
Ni	O site	0.00	0.16	4.6
Ni	hollow site	1.04	1.06	6.0
Ni	Mg site	1.40	1.66	5.0
Co	O site	2.68	2.78	6.9

TABLE III. Net charge of Ni atom and its nearest-neighbor O and Mg atoms according to Bader analysis. Ag/MgO is the bare slab without adatoms. These results were obtained from all-electron LAPW calculations.

	GGA			GGA+U		
	Ni	O_{nn}	Mg_{nn}	Ni	O_{nn}	Mg_{nn}
O site	−0.17	−1.50	+1.72	−0.13	−1.52	+1.71
hollow site	+0.38	−1.51	+1.71	+0.43	−1.54	+1.71
Mg site	−0.26	−1.62	+1.68	−0.40	−1.61	+1.69
MgO/Ag		−1.64	+1.71			

neighbor Mg and O atoms, as well as for a bare slab of MgO/Ag. Because this analysis includes the interstitial electrons, these results can provide insight on the nature of the bonding between the adatom and the surface. On the O site, the Ni adatom gains electrons from its O neighbor (which is less negatively charged than it would be on bare MgO/Ag). In contrast, on the hollow site, Ni loses electrons to the underlying Ag substrate. These charge transfer results are relatively insensitive to local Coulomb interactions.

To understand the site dependence of the Ni moment, we examine the bonding and electronic density of states, starting with Ni on the O site within GGA. While the transfer of electrons from the substrate to a $3d^9 4s^1$ configuration can only reduce the spin moment, the gain of ~ 0.2 is not enough to account for the full quenching of the moment. The fact that most of the electrons are transferred from the neighboring O atom, and the fact that Ni adsorption causes the O atom to displace upwards out of the MgO ML (Table I), suggest the formation of a covalent bond. Indeed, previous studies of Ni on MgO discuss a bonding mechanism involving Ni hybrid orbitals of $4s$ and d_{z^2} character.[5–8,11] One of the two orthogonal orbitals, which we denote as $4s{+}d_{z^2}$, is oriented perpendicular to the surface and interacts strongly with O p_z orbitals, forming a bonding combination (mostly O p_z) about 6 eV below the Fermi level (E_F) and an antibonding combination (mostly Ni $4s{+}d_{z^2}$) about 1 eV above the Fermi level. This can be seen in the electronic density of states plotted in Fig. 3(a). The other hybrid orbital, denoted $4s{-}d_{z^2}$, is concentrated in the plane parallel to the surface, and hence interacts much more weakly with the surface. This planar hybrid orbital lies just below the other Ni d states, about 1 eV below the Fermi level. The covalent interaction between Ni and O pushes the antibonding orbital high enough to be unoccupied in both spin channels, so the other d and s-d hybrid orbitals are fully occupied, yielding a zero net spin.

When the orbital-dependent Coulomb interaction U is included within GGA+U, the density of state changes significantly since the d and s states are affected differently. The hybridization between Ni d_{z^2} and s orbitals weakens, and the interaction between these orbitals and O p states is affected. The partial density of states plots in Fig. 3(b) show the majority and minority spin d_{z^2} orbitals split by about 4 eV ($\sim U$). The antibonding Ni - O orbital, now mostly composed of Ni s states, has a small spin splitting of the opposite polarity: the spin-down states lie just below E_F and the spin-up ones lie just above E_F. Hence even though U induces a moment in the d shell within the Ni muffin tin, this moment is screened by the oppositely polarized antibonding orbital formed from Ni $4s$ and O $2p_z$ orbitals. This is illustrated in Fig. 4(a), which shows a majority-spin (red) isosurface with d_{z^2} character on the Ni atom, surrounded by the antibonding Ni s - O p_z minority-spin (blue) isosurface (corresponding to minority spin states near $\sim -0.5\ eV$ in Fig. 3(b)). The total magnetization of the system remains close to zero.

The situation differs for the hollow site. The presence of the Ni at the hollow site disrupts the MgO bond network, and the two O atoms that neighbor the Ni atom are displaced out of the surface by nearly 0.5 Å to form bonds with the Ni, as is evident in Fig. 4(b). The resulting polar covalent Ni-O bond length is only about 6% larger than the corresponding O-site bond (Table I). The hollow site has C_{2v} symmetry, meaning that the d_{xz}, d_{yz} degeneracy is broken. The lobes of the d_{yz} orbital point towards the O neighbors and interact with O p_y orbitals. However, since d_{yz} transforms differently than $4s$, symmetry considerations prevent the d_{yz} orbital from forming diffuse hybrids with $4s$ analogous to the $4s{\pm}d_{z^2}$ orbitals on the O site that enhance the orbital overlap between the adatom and surface atoms. While symmetry permits hybridization between Ni s and $d_{x^2-y^2}$ orbitals, the hybrid that interacts strongly with O p states has mostly Ni s character, while the orthogonal hybrid orbital is mostly Ni $d_{x^2-y^2}$. Hence the Ni d orbitals all retain a higher degree of localization than they do on the O site. Within GGA, it becomes favorable for the antibonding Ni d_{yz} - O p orbitals to become spin polarized and this largely accounts for the total moment of about 1 μ_B. This can be seen in Fig. 3(c).

Because the effect of U in the hollow site case is to increase the splitting between the d_{yz} majority and minority spin states, the occupation of s and d states and the total moment are not significantly impacted, as can be seen in Fig. 3(d). Figure 4(b) shows the spin density for this case. The majority-spin isosurface in red has antibonding Ni d_{yz} - O p_y character. While it is hard to see from the angle shown, the minority-spin isosurface in blue has the character of a $4s{-}d_{x^2-y^2}$ hybrid.

We return now to the question of why the local Coulomb interaction stabilizes the hollow site relative to the O site. When Ni adsorbs to the O site it forms a strong covalent bond with O through diffuse sd hybrids that overlap significantly with O p orbitals. Since the orbital-dependent U disrupts the sd hybridization, it weakens the binding of the Ni to the O. On the hollow site, geometric and symmetry considerations prevent the formation of diffuse sd hybrids that overlap strongly with O, so the impact of U, both in terms of binding energy and spin moment, is smaller. As a result, increasing the

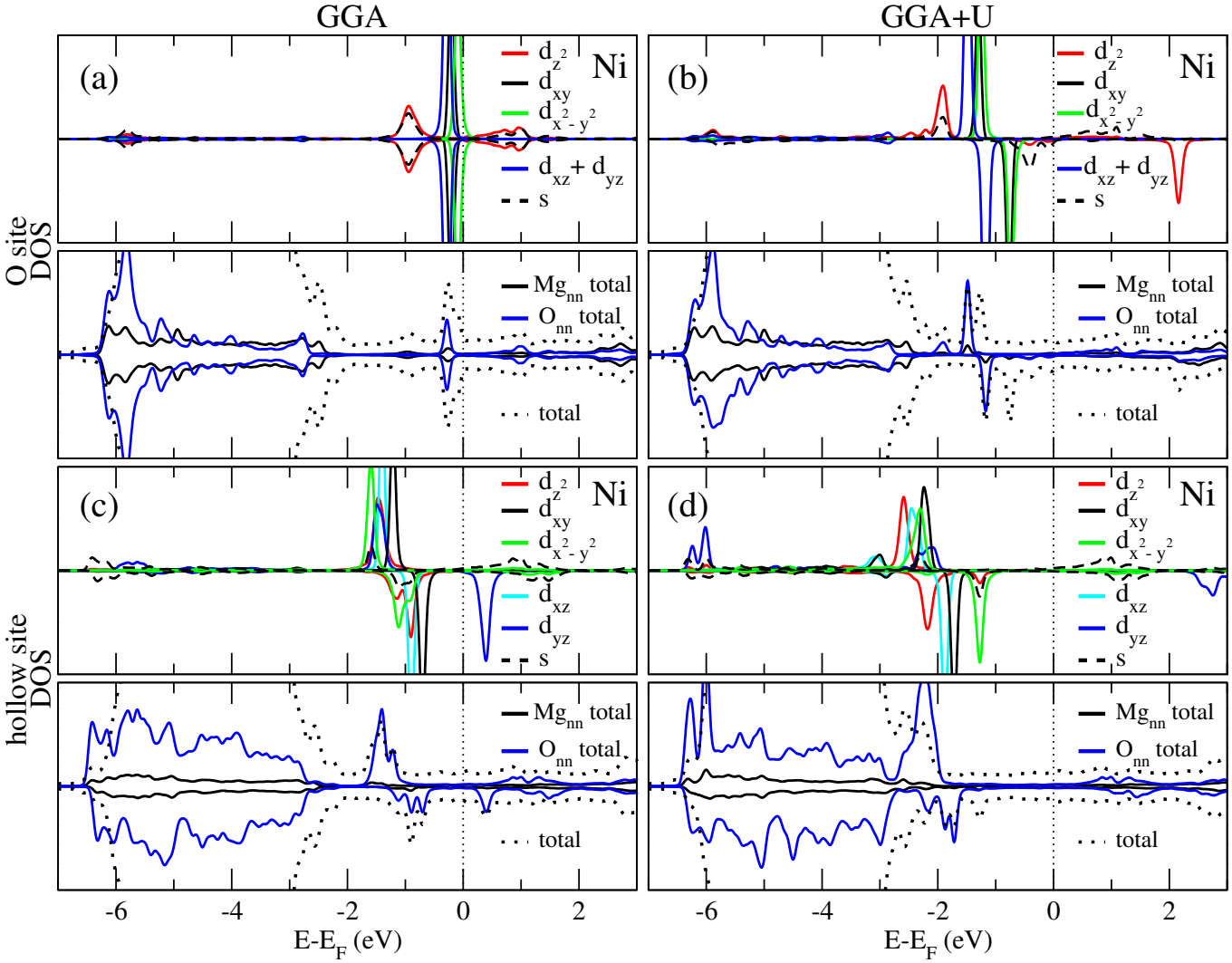

FIG. 3. (Color online) Densities of states from inside the muffin-tins of all-electron LAPW calculations. (a) GGA results for Ni on O site. (b) GGA+U results for Ni on O site. (c) GGA results for Ni on hollow site. (d) GGA+U results for Ni on hollow site. In all graphs, majority spin is plotted on the positive ordinate and minority spin on the negative ordinate. Total DOS has been scaled down significantly, and includes contributions from the interstitial region. The relative scales of nearest-neighbor Mg and O, as well as Ni s and d DOS have been adjusted to enhance viewability.

strength of the local Coulomb interaction decreases the stability of the O site relative to the hollow site.

The presence of magnetization in adatoms depends largely on the relative strengths of the covalent interaction with surface atoms and the intra-atomic exchange coupling for the adatom. In a previous study,[4] our calculations found that Co adsorbs to the O site of the MgO/Ag surface. We also found that, in contrast to Ni, it maintains a magnetization close to the atomic value (Table II). This can be explained by differences in the Ni-O and Co-O interactions. Unlike Ni, Co remains charge neutral when adsorbed, according to a Bader analysis, and the neighboring O and Mg atoms displace downward rather than being attracted to the adatom (Table I). Since the s-d transition energy is larger in Co than Ni, the hybridization between s and d orbitals is reduced, leading to less interatomic overlap and weaker covalent interactions. The d orbitals remain localized enough to support magnetism.

IV. CONCLUSIONS

Using first-principles calculations, we have found a strong site dependence of the electronic and magnetic properties of Ni on MgO/Ag. In particular, the magnetic moment varies from S = 0 to nearly 1 as Ni is moved away from surface O. This is in stark contrast with the situation of Co on MgO/Ag, in which the O site facilitates the preservation of Co spin and orbital moments on the

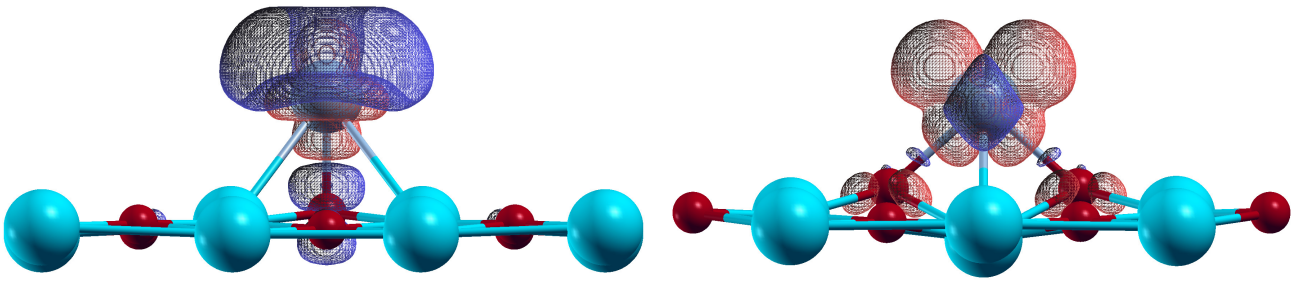

(a) O site (b) hollow site

FIG. 4. (Color online) Spin density isosurfaces of Ni adsorbed on MgO/Ag, from GGA+U all-electron LAPW calculations. Red and blue surfaces correspond to majority and minority spin densities of 0.00175 e/a.u.^{3}, respectively. (a) O site: the majority spin d_{z^2} is screened by the antibonding Ni s - O p orbital. (b) hollow site: the antibonding Ni d_{yz} - O p orbital is spin polarized. The y axis is parallel to the line joining the two O atoms that neighbor the Ni. These two O atoms are vertically displaced out of the MgO plane. O atoms are represented by small red spheres.

surface.

Furthermore, we see that the energy surface for adsorption of Ni on MgO/Ag is very different from that for Ni on MgO. On MgO/Ag, the O site and hollow site are competitive in energy, and it is not clear from theory alone which site will be realized in experiments. However, the properties of the Ni adatom on the two sites differ significantly, not just in the magnetic moment, but also in the charge transfer and bonding.

The energetic proximity of the hollow and O sites raises the interesting possibility of being able to select one site or the other, and tune the magnetic moment by modification of the substrate through, for example, application of strain or introduction of defects. It would also be interesting to compare bilayer and monolayer MgO on Ag experimentally. The bilayer would be much more rigid than the monolayer, and hence we would expect the O site to be clearly favored for Ni adsorption.

ACKNOWLEDGMENTS

The authors thank Shruba Gangopadhyay, Susanne Baumann and Andreas Heinrich for fruitful discussions. This work was supported in part by NSF Grants DMR-1006605 & EFRI-143307. BAJ acknowledges the Aspen Center for Physics and the NSF Grant PHY-1066293 for hospitality during the writing of this paper.

* ora@georgetown.edu

[1] L. Néel, Ann. géophys **5**, 99 (1949).
[2] C. F. Hirjibehedin, C.-Y. Lin, A. F. Otte, M. Ternes, C. P. Lutz, B. A. Jones, and A. J. Heinrich, Science **317**, 1199 (2007).
[3] S. Loth, S. Baumann, C. P. Lutz, D. M. Eigler, and A. J. Heinrich, Science **335**, 196 (2012).
[4] I. G. Rau, S. Baumann, S. Rusponi, F. Donati, S. Stepanow, L. Gragnaniello, J. Dreiser, C. Piamonteze, F. Nolting, S. Gangopadhyay, O. R. Albertini, R. M. Macfarlane, C. P. Lutz, B. A. Jones, P. Gambardella, A. J. Heinrich, and H. Brune, Science **344**, 988 (2014).
[5] I. Yudanov, G. Pacchioni, K. Neyman, and N. Rösch, J. Phys. Chem. B **101**, 2786 (1997).
[6] K. Neyman, S. Vent, G. Pacchioni, and N. Rösch, Il Nuovo Cimento D **19**, 1743 (1997).
[7] N. López and F. Illas, J. Phys. Chem. B **102**, 1430 (1998).
[8] A. Markovits, M. K. Skalli, C. Minot, G. Pacchioni, N. López, and F. Illas, J. Chem. Phys. **115**, 8172 (2001).
[9] A. Markovits, J. C. Paniagua, N. López, C. Minot, and F. Illas, Phys. Rev. B **67**, 115417 (2003).
[10] K. Neyman, C. Inntam, V. Nasluzov, R. Kosarev, and N. Rösch, Appl. Phys. A **78**, 823 (2004).
[11] S. Fernandez, A. Markovits, F. Fuster, and C. Minot, J. Phys. Chem. C **111**, 6781 (2007).
[12] Y. Dong, S. Wang, Y. Mi, Y. Feng, and A. Huan, Surface Science **600**, 2154 (2006).
[13] P. Blaha, K. Schwarz, G. Madsen, D. Kvasnicka, and J. Luitz, *WIEN2k, An Augmented Plane Wave + Local Orbitals Program for Calculating Crystal Properties (Karlheinz Schwarz, Techn. Universität Wien, Austria)* (2001) ISBN 3-9501031-1-2.
[14] P. E. Blöchl, Phys. Rev. B **50**, 17953 (1994).
[15] G. Kress and J. Furthmüller, Comput. Mater. Sci **6**, 15 (1996).
[16] J. P. Perdew, K. Burke, and M. Ernzerhof, Phys. Rev. Lett. **77**, 3865 (1996).
[17] G. K. H. Madsen and P. Novák, EPL (Europhysics Letters) **69**, 777 (2005).
[18] S. L. Dudarev, G. A. Botton, S. Y. Savrasov, C. J. Humphreys, and A. P. Sutton, Phys. Rev. B **57**, 1505 (1998).

[19] All-electron LAPW calculations used $R_{mt}K_{max} = 7$, where R_{mt} is the smallest muffin-tin radius in the unit cell, for all calculations. Structural relaxations were carried out with k-point meshes of $6 \times 6 \times 1$ and finite temperature smearing of 0.001 Ry. Denser k-point grids of up to $19 \times 19 \times 1$ were used for more accurate magnetic moments and densities of states. VASP calculations were carried out using a plane-wave cutoff of 500 eV, k-point sampling of $8 \times 8 \times 1$ grids, and a Gaussian smearing width of 0.02 eV.

[20] J. Repp, G. Meyer, S. M. Stojković, A. Gourdon, and C. Joachim, Phys. Rev. Lett. **94**, 026803 (2005).

[21] S. Baumann, I. G. Rau, S. Loth, C. P. Lutz, and A. J. Heinrich, ACS Nano **8**, 1739 (2014), PMID: 24377286.

[22] T. O. Wehling, A. I. Lichtenstein, and M. I. Katsnelson, Phys. Rev. B **84**, 235110 (2011).

[23] U. Litzén, J. W. Brault, and A. P. Thorne, "Spectrum and term system of neutral nickel: Ni I," NIST Atomic Spectra Database (ver. 5.2), [Online]. Available: `http://physics.nist.gov/asd` [2014, November 7]. National Institute of Standards and Technology, Gaithersburg, MD. (2014).

[24] R. F. W. Bader, "Atoms in molecules," in *Encyclopedia of Computational Chemistry* (John Wiley & Sons, Ltd, 2002).